

## RESEARCH ARTICLE

# Design and realization of transparent solar modules based on luminescent solar concentrators integrating nanostructured photonic crystals

Alberto Jiménez-Solano<sup>1</sup>, José-Maria Delgado-Sánchez<sup>2</sup>, Mauricio E. Calvo<sup>1</sup>, José M. Miranda-Muñoz<sup>1</sup>, Gabriel Lozano<sup>1</sup>, Diego Sancho<sup>2</sup>, Emilio Sánchez-Cortezón<sup>2</sup> and Hernán Míguez<sup>1\*</sup>

<sup>1</sup> Multifunctional Optical Materials Group, Instituto de Ciencia de Materiales de Sevilla, Consejo Superior de Investigaciones Científicas-Universidad de Sevilla (US-CSIC), Américo Vespucio 49, 41092 Sevilla, Spain

<sup>2</sup> Abengoa Solar New Technologies S.A., Parque Empresarial Soland, Ctra. A472 km6, 41800 Sanlúcar la Mayor, Sevilla, Spain

## ABSTRACT

Herein, we present a prototype of a photovoltaic module that combines a luminescent solar concentrator integrating one-dimensional photonic crystals and in-plane CuInGaSe<sub>2</sub> (CIGS) solar cells. Highly uniform and wide-area nanostructured multilayers with photonic crystal properties were deposited by a cost-efficient and scalable liquid processing amenable to large-scale fabrication. Their role is to both maximize light absorption in the targeted spectral range, determined by the fluorophore employed, and minimize losses caused by emission at angles within the escape cone of the planar concentrator. From a structural perspective, the porous nature of the layers facilitates the integration with the thermoplastic polymers typically used to encapsulate and seal these modules. Judicious design of the module geometry, as well as of the optical properties of the dielectric mirrors employed, allows optimizing light guiding and hence photovoltaic performance while preserving a great deal of transparency. Optimized in-plane designs like the one herein proposed are of relevance for building integrated photovoltaics, as ease of fabrication, long-term stability and improved performance are simultaneously achieved. Copyright © 2015 John Wiley & Sons, Ltd.

## KEYWORDS

luminescent solar concentrator; photovoltaic module; photonic crystal

### \*Correspondence

Hernán Míguez, Multifunctional Optical Materials Group, Instituto de Ciencia de Materiales de Sevilla, Consejo Superior de Investigaciones Científicas-Universidad de Sevilla (US-CSIC), Américo Vespucio 49, 41092 Sevilla, Spain.

E-mail: h.miguez@csic.es

Received 21 October 2014; Revised 1 March 2015; Accepted 18 March 2015

## 1. INTRODUCTION

Luminescent solar concentrators (LSCs) [1] have been the subject of intense research during the last three decades [2,3]. From a technological perspective, they offer a promising route towards see-through solar modules of potential use as photovoltaic windows with architectural applications [4,5]. In its most typical realization, solar light impinges on a flat semi-transparent layer doped with a dye capable of absorbing part of the incoming solar frequencies. By a process of luminescence, the absorbed energy is converted into lower frequencies photons that are emitted and guided by total internal reflection towards a set of thin-film solar cells that are

placed perpendicular to the surface of the film. In this configuration, all photons travelling along the slab reach the surface of the adjacent thin-film solar cells. From a fabrication point of view, however, it would be more convenient to have the solar cells located on the same substrate than the luminescent film rather than orthogonal to it. A coplanar configuration eases manufacturing as it does not require fine and precise handling and positioning of the cells on the edge of the slab acting as a planar waveguide. In this regard, very few designs with this specific configuration have been reported [6], none of them showing an optimization of the light guiding efficiency.

Herein, we prepare a semi-transparent solar cell module, for photovoltaic windows, in which thin-film solar

cells are located in-plane with the luminescent concentrator. The performance of the solar concentrator is enhanced by coupling the luminescent film to nanostructured photonic crystals that enhance simultaneously light absorption at shorter wavelengths and light guiding at longer ones. The porous nature of such mirrors favours the integration with the luminescent film, hence reducing the effective thickness of the device and allowing a larger number of photons to reach the thin-film solar cells, in good agreement with optimized models of the basic module based on ray optics. Optimized modules integrating one-dimensional photonic crystals (1DPC) present incident to guided photon efficiencies around 28% higher than those in which no optical materials are employed to improve light harvesting and guiding. All techniques and designs herein employed are amenable to mass production.

## 2. DISCUSSION

### 2.1. Device and model description

In our module, we employ a 2- $\mu\text{m}$ -thick luminescent layer made of a perylene dye (Lumogen F Red 305 BASF) embedded within a poly methyl methacrylate (PMMA) matrix. This layer is in turn sandwiched between two 0.5-mm-thick layers of ethyl vinyl alcohol (EVA), which serve both to improve adhesion to the two 4-mm-thick glass covers and as a refractive index matching compound. CIGS solar cells are deposited onto one of the glass substrates with their active surfaces facing upwards. In this way, in the final structure, the photovoltaic devices are coplanar with the luminescent slab. The module works absorbing part of the incoming light in the luminescent slab, which emits photons of longer wavelengths isotropically. Because of the phenomenon of total internal reflection, part of the light emitted by the luminescent slab undergoes successive reflections at the glass–air interfaces. Finally, guided light reaches the edges of the luminescent layer and either encounters the coplanar solar cells or, if the angle of internal reflection is too high, escapes through the laterals. Our calculations estimate that a coplanar design collects 34% of the light that would be harvested by an orthogonal one. However, this number can be greatly enhanced by introducing optical nanostructures, as it will be shown in the succeeding text.

From a materials perspective, perylene molecules embedded in PMMA show a nominal quantum yield of 85% (ratio between the number of absorbed and emitted photons). They are in a concentration of 3% in the PMMA film, which provides an absorptance,  $A$ , band centered at around 576 nm with a maximum  $A_{\text{max}} = 90\%$ . Higher concentrations would lead to stronger absorption but also to quenching of the luminescence. This compromise implies that a certain percentage of incident photons will pass unaffected by the slab, being the first source of losses found in a luminescent concentrator. Another common cause of low efficiency in LSC is the loss of emitted energy through

the light escape cone, resulting from circumrotating the line that forms an angle equal to  $\theta = \arcsin(n^{-1})$  with the normal to the LSC surface. The angle  $\theta$ , measured with respect to the surface normal, is the critical angle above which total internal reflection occurs, and  $n$  is the refractive index of the planar waveguide. Among emitted photons, those travelling with directions comprised within such exit cone have a high probability of being lost by transmission. Note that a photon emitted within the escape cone can be reabsorbed by the dye and reemitted outside of this cone. As in our case the refractive index of our glass is 1.50 these losses were estimated to be 25% of total emitted light. This figure is given by the ratio of the solid angle subtended by the critical angle and the one subtended by a hemisphere. Figure 1(a) shows a scheme of the module as well as examples of all the possible ends for an incoming photon.

We have analysed the effect of integrating a dielectric mirror, also known as distributed Bragg reflector or 1DPC, on the amount of light guided by the LSC and eventually harvested by the thin-film solar cells. Our approach is inspired by previous works in which dichroic mirrors were deposited on the surface of the luminescent slabs to enhance selectively the reflection of emitted wavelengths at angles comprised within the escape cone [7]. In this way, all emitted photons are, in principle, confined within the glass acting as a planar waveguide. In our case, we target light both unabsorbed by the dye and that emitted at directions comprised within the escape cone or lost through the lateral edges. We consider mirrors made of a periodic structure of alternated nanoparticle-based porous titania and silica layers, possessing refractive indexes of  $n_{\text{H}} = 1.95$  and  $n_{\text{L}} = 1.37$ , respectively. These materials were chosen as they yield highly reflecting mirrors [8] after a simple and fast processing from liquid phase precursors at room temperature. In Figure 1(b), we show a generic scheme of the module integrating photonic crystal mirrors in different positions.

In order to find the structure and the position relative to the emitting layer in the device of the photonic multilayers that maximize the efficiency of the module, we use a code written in Fortran and MatLab that combines a ray optics approach, in which we account for the probability of each possible event (transmission, reflection, absorption, emission, guiding, reabsorption, reemission and so on) using a Monte Carlo approach [7,9,10], with a vector wave transfer matrix approach, to describe the optical properties of the different multilayer dielectric mirrors considered. The trajectories of all photons reaching the module are simulated. The figure of merit employed to perform the optimization is the ratio between the number of photons reaching the solar cells and those impinging on the LSC. As a reference, a bare luminescent solar concentrator module was used, that is, not integrating any type of dielectric mirror. A study of the geometrical parameters that gave rise to the optimized performance of such reference was first carried out. Then, the effect of integrating a dielectric multilayer mirror at the different interfaces of the module was evaluated.

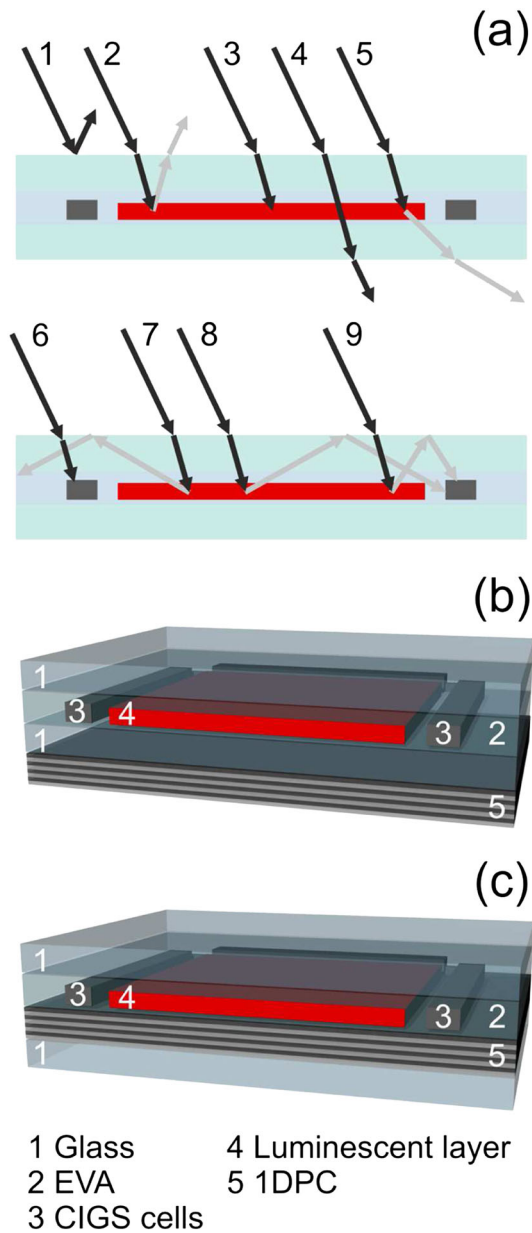


**Figure 1.** (a) Scheme of the basic coplanar module with examples of all the possible ends for an incoming photon, which can be (1) specularly reflected; (2) diffusely reflected; (3) absorbed by the fluorophore; (4) ballistically transmitted; (5) diffusely transmitted; (6) absorbed by the cell directly; (7) lost at the module's edge; (8) lost at the non-active face of the cell; and finally, (9) absorbed by the cell after being guided by the luminescent solar concentrator. (b)–(c) Schemes of the two designs considered. In the 'external' configuration, the photonic crystal is fabricated in the outer side of the rear glass substrate (b). In the 'integrated' configuration, the photonic crystal is grown between the active layer of the device and the rear glass substrate (c). EVA, ethyl vinyl alcohol; 1DPC, one-dimensional photonic crystals.

In all cases, we considered a maximum number of 15 constituent layers for each mirror, for the sake of manufacturability.

## 2.2. Photonic multilayer integration

With these restrictions, we first obtained the mirror structures whose reflectance best matched either the absorption or the emission spectra of the perylene embedded in PMMA. In Figure 2(a), we plot the absorbance and

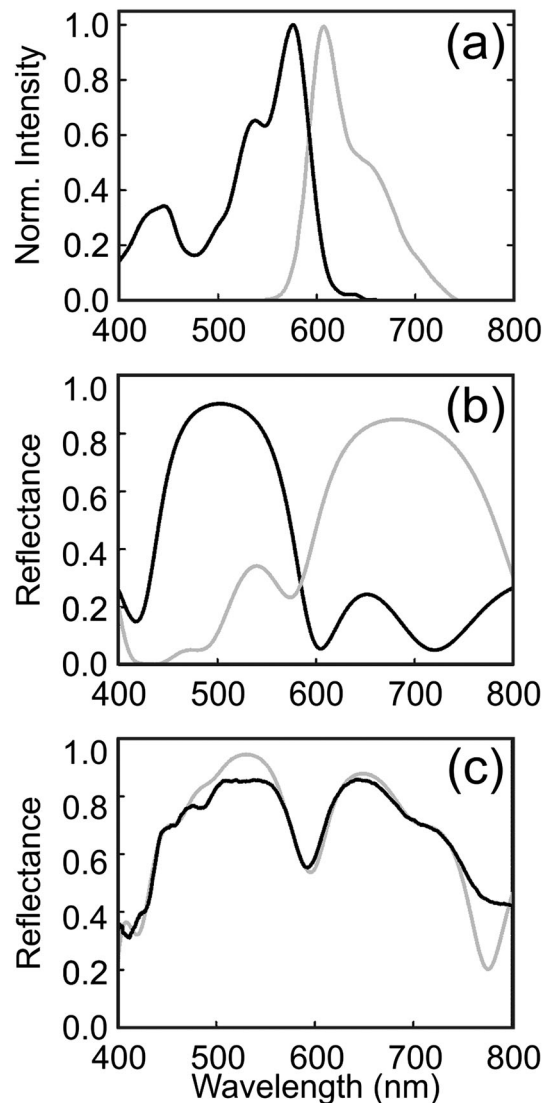


**Figure 2.** (a) Absorbance (black) and photoluminescence (grey) spectra of perylene embedded in poly methyl methacrylate film. (b) Theoretical reflectance spectrum of the photonic crystals designed to overlap with the absorption (black) and the emission bands (grey) of the emitting material. (c) Experimental (black) and theoretical (grey) reflectance spectra of a multilayered structure made of the stack of the two dielectric mirrors shown in (b). It matches the absorption and the emission of the fluorophore simultaneously.

photoluminescence spectra of the perylene dye employed to build the module. Absorbance was measured from transmission measurements realized in an ultraviolet–visible spectrophotometer (Shimadzu), while the emission spectra was attained using a double monochromator spectrofluorimeter (Fluorolog-3 Horiba Jobin Yvon) fixing the excitation wavelength  $\lambda = 440$  nm. In Figure 2(b), the calculated spectra for the optimized mirrors are plotted. Please notice that an intense primary reflectance maximum is attained as a result of the interference between the beams partially reflected at each interface within the photonic crystal. Also, secondary reflectance maxima arise as a result of the interference between the beams reflected at the top and bottom surfaces of the mirror. Such secondary lobes are responsible for a null or even deleterious effect on the efficiency of the module when a mirror designed for reflecting the emitted wavelength range is deposited at the front air–glass interface. The reason is that, although the primary maximum reflects back into the module-emitted photons, secondary reflectance lobes prevent part of the incoming photons with frequencies comprised in the absorption band of the dye to reach the luminescent layer. These two effects cancel each other out, and as a result, the module is not improved. On the other hand, a clear improvement is predicted by our theoretical model when a dielectric mirror capable of reflecting either unabsorbed photons or emitted photons is located at any position behind the luminescent layer with respect to the direction of incoming light. In that regard, best results are attained when the emitted frequency-selective back reflectors are placed as close as possible to the luminescent layer (Figure 1(c)), rather than in the outer surface of the glass substrate (Figure 1(b)). This preferred location effectively reduces the thickness of the concentrator, as light is now guided between the upper air–glass interface and that is created between the luminescent slab and the photonic crystal. By doing so, the period of the light ray rebound caused by internal reflection is shorter and the probability of hitting the coplanar solar cell surface increases. Indeed, our calculations estimate that the number of guided photons harvested by the CIGS cells increases by a factor of 1.8 when a photonic multilayer like the one herein employed is integrated in the module. On the other hand, if a photonic crystal designed to reflect unabsorbed photons back into the PMMA-embedded perylene film is used, an increase of the efficiency of the module is also predicted. The optimized design thus includes both types of mirrors located at the back of the LSC. The calculated reflectance of the optimized mirror design, always restricted to 15 layers, is plotted in Figure 2(c) (grey solid line). Note that this photonic multilayer is made of the stack of two mirrors, each one having a different unit cell.

Realization of this optimized design was carried out by depositing a multilayer dielectric mirror structure capable of reflecting both unabsorbed light and that emitted in directions comprised within the escape cone back to the LSC. The experimental specular reflectance at normal incidence, measured using a spectrophotometer attached to a

microscope (Bruker IFS66), is plotted in Figure 2(c) (black solid line), in which a good agreement between the designed and realized reflectance can be observed. Apart from the advantage that location of this specific mirror location implies from the perspective of the optical design, it also favours the stability of the enhanced performance module: as it is placed in direct contact with the EVA polymer that embeds the luminescent layer, the bottom sealing glass protects both the emitter and the mirror, preventing their degradation and ensuring the durability of the module. Also, the void nanostructured network of the multilayer allows diffusion of EVA all through the mirror, without loss of optical quality. In this way, the dielectric mirror enables the bonding between EVA and PMMA, on one side, and between EVA and the glass substrate, on the other, and hence does not diminish the mechanical stability of the ensemble. In Figure 3, a field emission scanning electron microscopy (FESEM) picture of the cross section of the photonic crystal-enhanced LSC is shown, the different types of layers being easily distinguishable.

Different sorts of optical analysis were performed in order to estimate the amount of light harvested and guided by the LSCs integrating the two-period photonic crystal mirror realized. Absorbance was estimated by collecting total transmittance and reflectance using an integrating sphere operating with synchronized entrance and exit monochromators (Fluorolog-3 Horiba Jobin Yvon). Re-illumination effects were accounted for by correcting the measurements with the spectra attained from the LSC irradiated with diffuse light from the same sphere [11]. This protocol provides reliable estimations of the absorbance spectrum of the different configurations. In Figure 4, the absorbance for the proposed design (black solid line) is plotted together with that of a reference module (grey line) for the sake of comparison. The light-harvesting enhancement observed (approximately 28%) is fairly close to that predicted by our model (33%).

The amount of light guided by the optimized configuration was also estimated. In order to do so, an experimental setup was mounted on an optical bench to measure the intensity of light exiting from the sides of a small prototype with the same characteristics than the designed LSC, but without

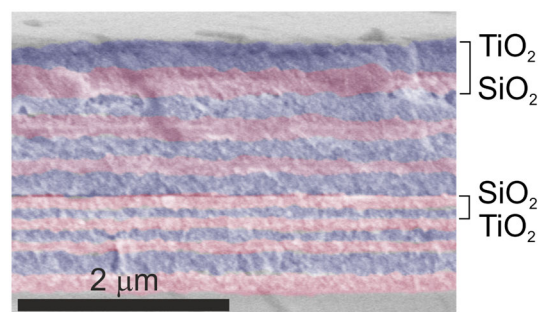


**Figure 3.** FESEM image of a cross section of a periodic multilayer structure made of two dielectric mirrors of different unit cell thickness, namely 160 and 190 nm.

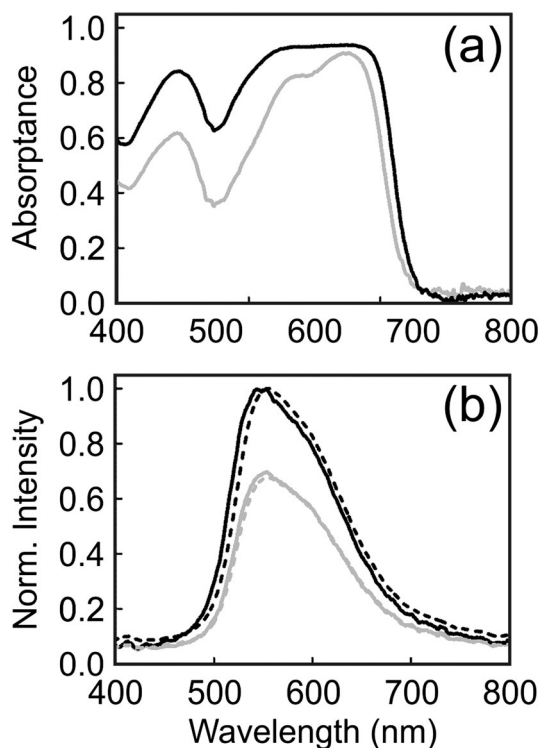


**Figure 4.** (a) Absorbance and (b) photoluminescence spectra collected from the side edges of a prototype that integrates a photonic multilayer (black line) and from a bare prototype (grey line). Calculations are also plotted in dashed lines.

any solar cell attached in order to facilitate the harvesting of light by a detector placed close to the edge. The spectrum of light emitted by the fluorophore and guided by the concentrator was collected with a spectrophotometer (Ocean Optics USB2000+) upon optical pumping with a fibre-coupled tunable laser (Fianium SC400). Excitation wavelength value was set to 500 nm. Sample was placed perpendicularly to the incident beam, and the detector was set to  $90^\circ$  in relation to the incident beam. Photoluminescence spectra collected from the side edges of the optimized and reference (without a photonic crystal attached) LSCs are plotted in Figure 4(b). The theoretically estimated spectra are plotted as well, fair agreement being found in this case as well. It can be clearly seen that, overall, the photonic crystal-based LSC gives rise to an important enhancement in the amount of guided light with respect to a bare LSC. It is important to notice that, once implemented in a module, not all this light is expected to reach the thin-film solar cell, as a result of the coplanar configuration of the surrounding cells.

### 2.3. Device performance analysis

Finally, these designs were implemented into the actual prototype modules. Please notice that the effect of the photonic crystal is not only to improve absorption of incoming radiation and guiding of emitted light in the LSC, but also

to change the colour of the semi-transparent window of the module, which might be of interest for decorative aspects in architectural applications. It should be mentioned that diverse techniques have been proposed to endow photovoltaic cells with colour [12–14]. In that regard, photonic crystal coatings offer a versatile approach to simultaneously select the colour and enhance the performance of the device. In Figure 5(a) and (b), the optimized module subject of analysis herein is shown in reflection and transmission mode, where the preservation of transparency after introducing our broad band frequency-selective dielectric mirror can be readily observed. Indeed, our design not only

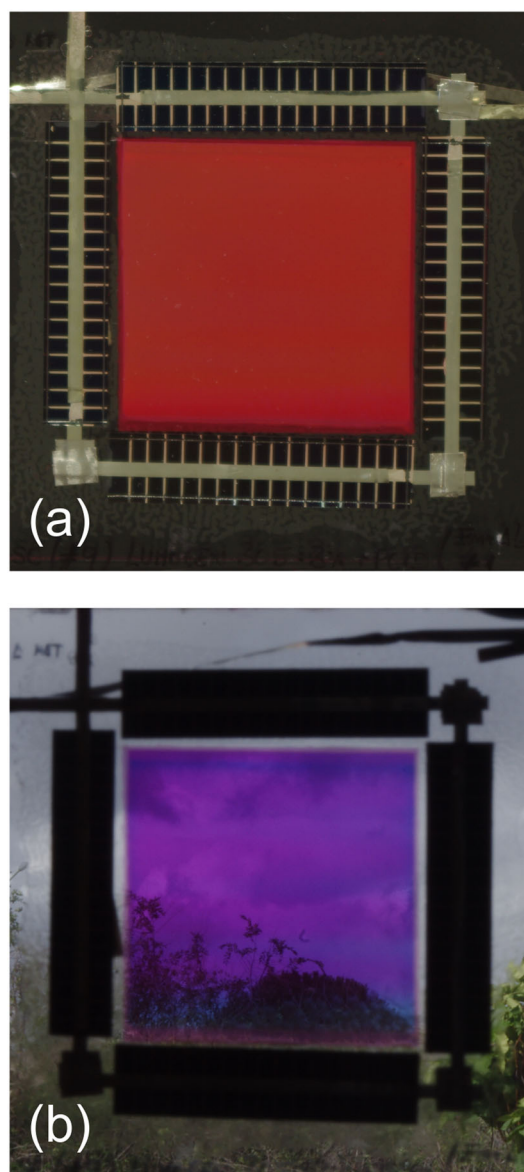


**Figure 5.** Digital camera pictures of a photovoltaic module that integrates an optimized photonic multilayer taken in (a) reflection and (b) transmission modes. For the former, a black background is used.

optimizes light guiding, but also partially keeps the transparency of the module, which is a necessity for applications in window panes. Following the rules ISO 9050:2003 (glazing in buildings) or IEC 82/691/NP (solar cells), which determines that the transparency of a film is determined, respectively, by either

$$\tau_g = \frac{\sum_{\lambda=380nm}^{780nm} T(\lambda)S(\lambda)V(\lambda)\Delta\lambda}{\sum_{\lambda=380nm}^{780nm} S(\lambda)V(\lambda)\Delta\lambda}$$

or

$$\tau_s = \frac{\sum_{\lambda=300nm}^{1100nm} T(\lambda)S(\lambda)\Delta\lambda}{\sum_{\lambda=300nm}^{1100nm} S(\lambda)\Delta\lambda}$$

where  $V(\lambda)$  is the photopic spectral luminous efficiency function that represents the wavelength-dependent sensitivity for an observer in photometry (ISO/CIE 10527),  $S(\lambda)$  corresponds to the solar spectral irradiance at the Earth surface after travelling through 1.5 times the atmosphere thickness (AM1.5) and  $T(\lambda)$  is the spectral transmittance of the sample, we obtain that the photonic crystal-enhanced LSC presents a transparency of  $\tau_s = 55\%$  (solar rule) or  $\tau_g = 28\%$  (architectonic rule), while the reference one possesses  $\tau_s = 88\%$  or  $\tau_g = 82\%$ , respectively. Note that, in contrast to the design herein proposed, previously optimized ones based on diffusive layers were typically opaque [15,16].

In Figure 6(a) and (b), the  $I$ - $V$  curves and the external quantum efficiency (EQE) of both the reference and the 1DPC-based devices are shown. The dimensions of the active area of the cells investigated are  $17 \text{ cm}^2$ . The power-conversion efficiency values are found to be 7.28% for the reference module under total illumination and 6.70% when only the CIGS cells are illuminated. The former value is 8.14% for the modules integrating photonic multilayers. Hence, when the whole module is illuminated (solar cells plus LSC), an improvement of the power-conversion efficiency of 12% is observed in the dielectric mirror-based LSC module with respect to the reference module and of 21% when compared with the performance of the four cells if illuminated while covering the LSC. If the contribution from the direct illumination of the solar cells is eliminated by concealing them, we observe a 69% increase of the short circuit photocurrent density in the dielectric mirror-based LSC with respect to a similar LSC that does not integrate a reflector. Also, when the EQE curves are compared, a clear increase is observed at all absorption wavelengths, as a result of the improved light guiding of the light generated after the subsequent recombination process. However, the EQE is more significantly reinforced at those frequencies for which absorbance is also increased. These results are in good agreement with the theoretical estimations for the ratio of photocurrent generated by the photonic crystal-based module divided by that of the reference when the cells are not directly illuminated (65%). Our results prove that coupling a thin multilayer coating to an LSC gives rise to a significant reinforcement of the photocurrent, and hence the power-conversion efficiency, as a result of the increase of both the absorption of incoming light and the optimized guiding of emitted photons. This

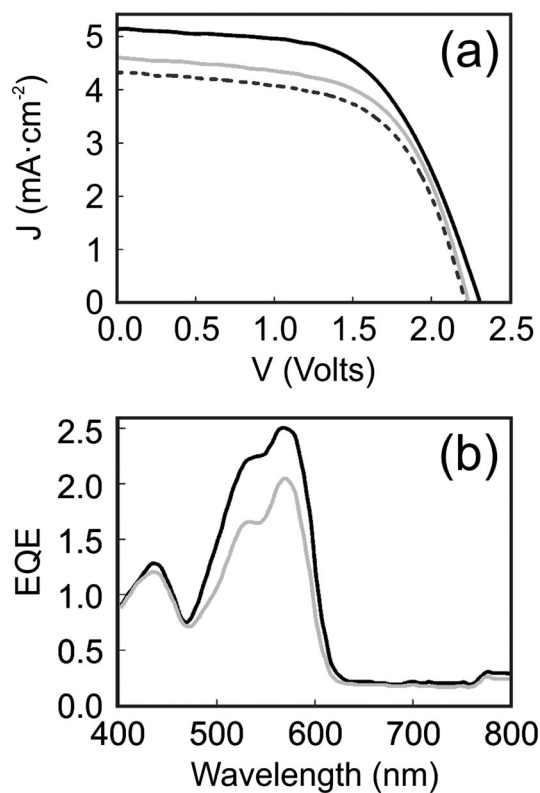


**Figure 6.** (a) Current density against voltage of total illumination of a photovoltaic module that integrates the photonic multilayer (black solid line) and a reference (grey solid line). For the sake of comparison, a direct illumination data is included (dashed line). (b) Spectral external quantum efficiency (EQE) obtained with the 1DPC integrated photovoltaic module (black solid line) and a reference (grey solid line).

increase in photocurrent with respect to the reference LSC is attained at the expense of decreasing its transparency. Although further improvement of the performance could be achieved by integrating reflectors made of a larger number of layers, the concomitant decrease of transparency must be considered if window applications are foreseen. Additional efforts should be performed to increase the transparent LSC area with respect to the opaque region of the module, occupied by the solar cells. Also importantly, preliminary tests performed outdoors indicate that the performance of the device remains uncompromised after several weeks of exposure to environmental conditions. In this regard, we could observe that encapsulation plays a key role to assure the long-term stability of the module. It should be remarked that, after finalizing these tests, the modules showed no degradation after several months of keeping them indoors. Finally, the question of whether or not our proposal may compete with currently available orthogonal designs, in which solar cells are placed on the glass slide edges, is also of relevance. By locating the photonic crystal mirror in contact with the luminescence thin film, we could increase the performance of the coplanar configuration with respect to the standard orthogonal

system from 34% to 62%. Our calculations show that by mirroring the glass sides, this ratio rises to 83%. Hence, our proposal may allow achieving a system almost as efficient as the orthogonal one, but with the advantage of presenting a much more simple manufacturing process.

### 3. CONCLUSIONS

We have presented an optimized design of a luminescent solar concentrator in which the solar cells are located coplanar with the luminescent layer. We have proven that integrating a photonic crystal mirror capable of reflecting back both unabsorbed photons and photons emitted by the luminescent dye in directions comprised within the escape cone provides a means to improve the power-conversion efficiency of the module through the simultaneous enhancement of the dyed layer absorptance and the guiding of emitted light. At the same time, a good extent of the original transparency is preserved, which makes the module amenable to be applied as a photovoltaic window. Our proposal is based on integrating porous nanostructured photonic crystals that give rise to both conformal contact with the polymer embedding the luminescent layer and favours the infiltration and bonding of the polymer that holds the different layers of the module together. We believe that the coplanar design herein analysed may ease the fabrication of LSC modules while improving their performance.

### ACKNOWLEDGEMENTS

The research leading to these results has been funded by the company Abengoa Solar New Technologies S.A. under a private contract with CSIC. Results herein presented are protected by the Spanish patent P201331748. HM is grateful for funding from the European Research Council under the European Union's Seventh Framework Programme (FP7/2007–2013)/ERC grant agreement no. 307081 (POLIGHT) and the Spanish Ministry of Economy and Competitiveness under grant MAT2011-23593. We also thank CITIUS for their valuable help with FESEM characterization.

### REFERENCES

1. Batchelder JS, Zewail AH, Cole T. Luminescent solar concentrators. I: theory of operation and techniques for performance evaluation. *Applied Optics* 1979; **18**(18): 3090–3110. DOI:10.1364/ao.18.003090.
2. Debije MG, Verbunt PPC. Solar concentrators: thirty years of luminescent solar concentrator research: solar energy for the built environment. *Advanced Energy Materials* 2012; **2**(1): 12–35. DOI:10.1002/aenm.201290003.
3. van Sark WGJHM, Barnham KWJ, Slooff LH, Chatten AJ, Büchtemann A, Meyer A, McCormack SJ, Koole R, Farrell DJ, Bose R, Bende EE, Burgers AR, Budel T, Quilitz J, Kennedy M, Meyer T, Donega CM, Meijerink A, Vanmaekelbergh D. Luminescent solar concentrators – a review of recent results. *Optics Express* 2008; **16**(26): 21773–21792. DOI:10.1364/oe.16.021773.
4. Chemisana D. Building integrated concentrating photovoltaics: a review. *Renewable and Sustainable Energy Reviews* 2011; **15**(1): 603–611. DOI:10.1016/j.rser.2010.07.017.
5. Meinardi F, Colombo A, Velizhanin KA, Simonutti R, Lorenzon M, Beverina L, Viswanatha R, Klimov V, Brovelli S. Large-area luminescent solar concentrators based on 'Stokes-shift-engineered' nanocrystals in a mass-polymerized PMMA matrix. *Nature Photonics* 2014; **8**(5): 392–399. DOI:10.1038/nphoton.2014.54.
6. Powell D, Alers G, Olson J. Luminescent solar concentrator apparatus, methods and applications, Patent WO 2012/061463.
7. Goldschmidt JC, Peters M, Prönneke L, Steidl L, Zentel R, Bläsi B, Gombert A, Glunz SW, Willeke GP, Rau U. Theoretical and experimental analysis of photonic structures for fluorescent concentrators with increased efficiencies. *Physica Status Solidi A* 2008; **205**(12): 2811–2821. DOI:10.1002/pssa.200880456.
8. Calvo ME, Colodrero S, Hidalgo N, Lozano G, Lopez-Lopez C, Sanchez-Sobrado O, Miguez H. Porous one dimensional photonic crystals: novel multifunctional materials for environmental and energy applications. *Energy Environmental Science* 2011; **4**(12): 4800–4812. DOI:10.1039/c1ee02081a.
9. Leow SW, Corrado C, Osborn M, Carter SA. Monte Carlo ray-tracing simulations of luminescent solar concentrators for building integrated photovoltaics. *Proceedings of the SPIE* 2013; **8821**: 882103.
10. Parel TS, Danos L, Fang L, Markvart T. Modeling photon transport in fluorescent solar concentrators. *Progress in Photovoltaics* 2014. DOI:10.1002/pip.2553.
11. Faulkner DO, McDowell JJ, Price AJ, Perovic DD, Kherani NP, Ozin GA. Measurement of absolute photoluminescence quantum yields using integrating spheres – which way to go? *Laser and Photonics Reviews* 2012; **6**(6): 802–806. DOI:10.1002/lpor.201200077.
12. Nicholson PG, Castro FA. Organic photovoltaics: principles and techniques for nanometre scale characterization. *Nanotechnology* 2010; **21**(49): 492001. DOI:10.1088/0957-4484/21/49/492001.
13. Klampaftis E, Richards BS. Improvement in multicrystalline silicon solar cell efficiency via addition of luminescent material to EVA encapsulation layer. *Progress in Photovoltaics* 2011; **19**(3): 345–351. DOI:10.1002/pip.1019.

14. Yang HJ, Chen CH, Lai WC, Wu CL, Huang CF, Chen YH, Hwang JC. Adjusted colorful amorphous silicon thin film solar cells by a multilayer film design. *Journal of the Electrochemical Society* 2011; **158**(9): H851–H853. DOI:10.1149/1.3604949.
15. Kim JM, Dutta PS. Optical efficiency–concentration ratio trade-off for a flat panel photovoltaic system with diffuser type concentrator. *Solar Energy Materials & Solar Cells* 2012; **103**: 35–40.
16. Sloof LH, Bende EE, Burgers AR, Budel T, Pravettoni M, Kenny RP, Dunlop ED, Büchtemann A. A luminescent solar concentrator with 7.1% power conversion efficiency. *Physica Status Solidi (RRL)* 2008; **2**(6): 257–259. DOI:10.1002/pssr.200802186.